Acta Materialia 196 (2020) 191–199

Contents lists available at ScienceDirect

Acta Materialia

journal homepage: www.elsevier.com/locate/actamat

Full length article

Off-stoichiometry effects on crystal nucleation and growth kinetics in soda-lime-silicate glasses. The combeite ($Na_2O•2CaO•3SiO_2$) – devitrite ($Na_2O•3CaO•6SiO_2$) joint

Guilherme S. Macena[a], Alexander S. Abyzov[b,c,*], Vladimir M. Fokin[a], Edgar D. Zanotto[c], Eduardo B. Ferreira[a]

[a] São Carlos School of Engineering, University of São Paulo, São Carlos, Brazil
[b] National Science Center "Kharkov Institute of Physics and Technology", Kharkov, Ukraine
[c] Department of Materials Engineering, Center for Research, Technology, and Education in Vitreous Materials, Federal University of São Carlos, São Carlos, Brazil

ARTICLE INFO

Article history:
Received 3 April 2020
Revised 5 June 2020
Accepted 20 June 2020
Available online 24 June 2020

Keywords:
Glass
Crystallization
Nucleation
Crystal growth
Soda-lime-silica
Devitrite
Combeite

ABSTRACT

To the present date, the vast majority of fundamental studies on glass crystallization has been carried out using stoichiometric compositions, whereas by far, the most common cases in glass technology are off-stoichiometric. In this work, we performed a comprehensive study on the nucleation and growth kinetics of combeite crystals in non-stoichiometric glasses of the combeite ($Na_2O•2CaO•3SiO_2$) – devitrite ($Na_2O•3CaO•6SiO_2$) system. Using cluster-size distribution functions based on a previously developed *kinetic model of nucleation*, we constructed the dependencies of the number $N(T)$ of nucleated and grown crystals on the nucleation time, t, and estimated the nucleation rates, $I(T) = dN(T)/dt$. We then cross-checked the theoretical calculations versus experimental data. In these calculations, the critical nucleus-supercooled liquid specific interfacial energy, σ, and the effective diffusion coefficient, D, were left as fitting parameters for the best possible description of experimental data. We show that as the precursor glass composition shifts from combeite to devitrite, and thus the difference of composition between the initial glass and the precipitated crystals increases, the interfacial energy increases, and the maximum steady-state nucleation rate, $I_{st}(T_{max})$, of combeite strongly drops. On the other hand, as a consequence of the composition shift, depending on the glass-forming system, the diffusion coefficient may increase or decrease. We also show a significant difference between D estimated from the nucleation experiments and D_u calculated from the growth rates. These results corroborate our previous studies on other systems and are relevant to elucidate the complex mechanisms of crystallization of non-stoichiometric glasses.

1. Introduction

Spontaneous crystallization must be avoided in glass fabrication. On the other hand, precise control is fundamental for making glass-ceramics (GCs), i.e., materials that are initially obtained as glass and are then partially crystallized by heat treatment, leading to polycrystalline articles with tailored microstructures and properties. Glass-ceramics were recently defined after a careful revision as "inorganic, non-metallic materials prepared by controlled crystallization of glasses via different processing methods. They contain at least one type of functional crystalline phase and a residual glass. The volume fraction crystallized may vary from ppm to almost 100%." [1]

Until now, the majority of fundamental research exploring glass-crystallization kinetic theories focused on congruent-melting compositions, i.e., systems with the same composition of the supercooled liquid and the precipitating crystal phase, also known as stoichiometric or polymorphic crystallization (e.g., Section 8.6 in [2]). However, to reconcile a minimal cost with a complex combination of properties demanded by the manufacturing processes, the vast majority of commercial glass and glass-ceramic wares yield devitrification phases with compositions very different from those of the precursor glasses [3] The difference of composition between the precipitating crystal and the parent glass may strongly affect the parameters controlling the nucleation and growth processes.

* Corresponding author at: National Science Center "Kharkov Institute of Physics and Technology", Kharkov, Ukraine.
E-mail address: abyzov@kipt.kharkov.ua (A.S. Abyzov).

https://doi.org/10.1016/j.actamat.2020.06.039
1359-6454/

Table 1
Nominal sample compositions (mol%).
(* used in nucleation and growth rate experiments).

Glass	Combeite	Devitrite	Na_2O	CaO	SiO_2
D0 *	100	0	16.67	33.33	50.00
D12.5	87.5	12.5	15.38	32.69	51.93
D25 *	75	25	14.29	32.14	53.57
D33 *	67	33	13.66	31.83	54.51
D50	50	50	12.50	31.25	56.25
D75	25	75	11.11	30.56	58.33
D100	0	100	10.00	30.00	60.00

For this reason, understanding and modeling the crystallization kinetics of non-stoichiometric glasses is an essential, intricate task. However, to the best of our knowledge, over the past 50 years, only a few works were devoted to the systematic study of non-stoichiometric glass crystallization (e.g. [4–15]). Of particular note are the comprehensive analysis of Narayan and Kelton [7] on the crystal nucleation in glasses of five compositions in the soda-lime-silica system, including the stoichiometric $Na_2O{\bullet}2CaO{\bullet}3SiO_2$, and the work by Gonzalez-Oliver and James [6] about the same system.

Examples of maximum-nucleation rate in the supercooled liquid of three silicate compositions, as a function of the composition of the precursor glass, are shown in Fig. 1. As expected, the maximum nucleation rate shows different behaviors, depending on the system, since changes in glass composition affect the three main parameters determining the crystal nucleation kinetics: the thermodynamic driving force, ΔG, the crystal/liquid interfacial energy, σ, and the kinetic barrier for critical nucleus formation, ΔG_D.

A non-monotonic change in the maximum nucleation rate of $Li_2O{\bullet}2SiO_2$ crystals as a function of Li_2O content in Li_2O-SiO_2 glasses is shown in Fig. 1a. A weak decrease in I_{max} with an increase in Li_2O followed by a sharp increase after 35 mol% Li_2O may be caused by an interplay between the kinetic and thermodynamic barriers for nucleation.

A significantly large amount of data, in conjunction with their in-depth analysis, is necessary to reveal the main effects controlling such behavior, as for the correlation of the maximum nucleation rate with the reduced glass transition temperature, reported in the literature [17]. In this work, we dig deeper into the effect of glass composition on the nucleation rate. We follow our recent publication [15] and expand the experimental dataset of the nucleation rate of combeite crystals in glasses of the soda-lime-silica system for compositions deviating from the stoichiometric combeite. This research represents a step forward towards understanding the general problem of crystal nucleation and growth kinetics in *off-stoichiometric* glasses.

2. Materials and methods

We prepared glasses of seven compositions, labeled as DX, where $0 < X < 100$ is the molar percent of devitrite in the $Na_2O{\bullet}2CaO{\bullet}3SiO_2$ (combeite)-$Na_2O{\bullet}3CaO{\bullet}6SiO_2$ (devitrite) joint of the soda-lime-silica system (Table 1). The compositions are plotted in Fig. 2, together with others mentioned in Fig. 1c. Lithium carbonate (Labsynth, 99.5%), calcium carbonate (Labsynth, 99.0%), and quartz (Vitrovita grade 3, 99.9%) were used as reagents. The batches of about 200 g were melted in an electrical furnace (CM Inc., USA), in a platinum crucible, between 1350 and 1400 °C for 3 h. The molten compositions were splat cooled between two steel plates to form thin, 1-3 mm glass pieces.

To estimate the characteristic temperatures, such as the glass transition T_g, and the liquidus T_L, we used differential scanning calorimetry (DSC 404 F1 Pegasus, NETZSCH, Germany). DSC analyses were performed for each composition using monolithic glass samples weighing approximately 20 mg heated at 10°C/min in platinum pans with lids in a synthetic air atmosphere.

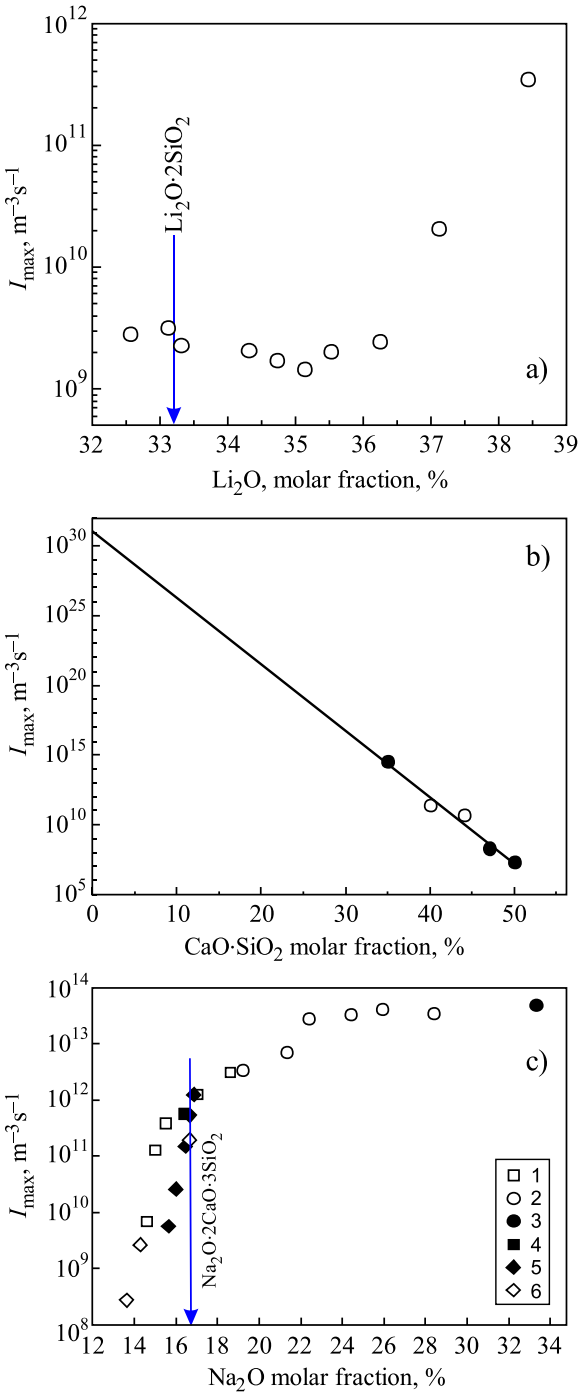

Fig. 1. Maximum nucleation rate (I_{max}) of a given crystalline phase as a function of composition in different systems: (**a**) $Li_2O{\bullet}2SiO_2$ in Li_2O–SiO_2 glasses [10]; (**b**) $Li_2O{\bullet}SiO_2$ in metasilicate glasses of the $CaO{\bullet}SiO_2$-$Li_2O{\bullet}SiO_2$ joint: black circles [13], open circles, this work; (**c**) $Na_2O{\bullet}2CaO{\bullet}3SiO_2$ in different soda-lime-silica glasses: *1*. CaO/SiO_2=2/3 [8], *2–4*. $CaO{\bullet}SiO_2$–$Na_2O{\bullet}SiO_2$ (*2*-[14], *3*-[16], *4*-[12]), respectively, *5*. $(Na_2O{\bullet}2CaO)(1\text{-}x) \bullet (3SiO_2)x$ [7], and *6*. $Na_2O{\bullet}2CaO{\bullet}3SiO_2$–$Na_2O{\bullet}3CaO{\bullet}6SiO_2$, this work. Despite the ratio of other components changes with the change in Na_2O mol%, the influence of the latter on the nucleation rate can be clearly traced.

The glass densities were estimated at room temperature using an analytical balance AX204 (Mettler Toledo) using the Archimedes principle.

The phases present in finely ground crystallized samples were determined by X-ray diffraction (XRD) using a diffractometer (Ul-

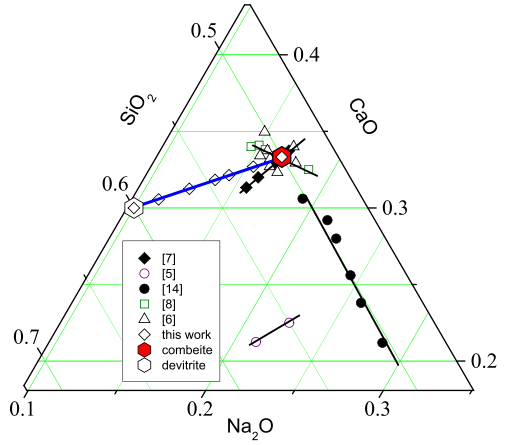

Fig. 2. Compositions of glasses used in this work, and compositions of other studies.

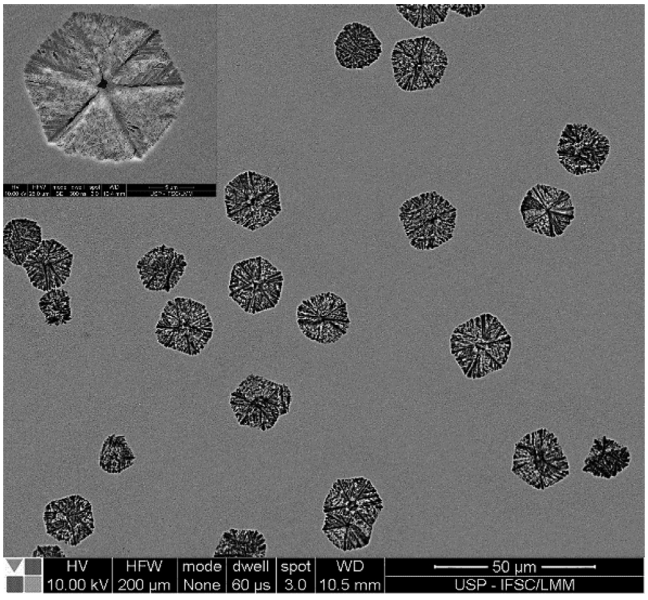

Fig. 3. SEM image of a cross-section of D33 glass sample subjected by heat treatments at T_n=600°C for 96 h and then at $T_d = 740$°C for 7 min.

tima IV, Rigaku, USA) with CuKα radiation (Fig. S1 in Supplementary material).

To detect the crystals nucleated at T_n we adopted the Tammann method, also known as the "development" method. This technique is suitable only when the temperature ranges of crystal nucleation and growth overlap only weakly, as in our case. For crystals nucleated at T_n to reach a visible size, they were subjected to a second treatment at $T_d > T_n$ to grow to a detectable size. The crystal nucleation I and growth U rates at T_d have to meet the following conditions: $I(T_d) \ll I(T_n)$ and $U(T_d) \gg U(T_n)$, as explained, e.g., in [18].

To estimate the volumetric number density, N, of developed crystals, the cross-section microstructure of treated samples was observed by reflected light microscopy (Leica DMRX with DFC490 CCD camera). Images were analyzed using stereology, by approximating the crystal cross-sections by circles, and taking their maximum radius, R. The number of crystals was then determined by $N = N_S/2R$, where N_S is the number of crystals in a sample cross section of area S (e.g. [19]). Using various images over the sample cross section, the mean and standard deviation of N were determined. Fig. 3 shows a polished cross-section of a heat treated sample. The underestimation of N due to the limited microscope resolution limit was also taken into account, but it was not higher than 5%. The average number of crystals counted for each nucleation time was not less than 300.

Commonly, nucleation experiments are analyzed in the Classical Nucleation Theory (CNT) framework based on a *kinetic model* for cluster formation [2]. To determine the nucleation rate and characteristic induction times, the proper analytical expressions derived as solutions of the Zeldovich-Frenkel equation (e.g., [2]) are fitted to experimental data of N versus nucleation time. In most cases, the "development" method adopted to study nucleation kinetics complicates the evaluation of the time-lags (see, e.g., [18]). To avoid this problem in this work, as well as in our recent publication [15], we used numerical calculations without the common approximation used in the derivation of analytical expressions for CNT. Several authors assume that the diffusion processes that control crystal nucleation and viscous flow are the same, and use viscosity data to analyze the nucleation kinetics. The next section provides a description of the method and the governing equations used here.

3. Governing equations

The numerical approach used here was described in [15], and in more detail in [2]. It is based on the calculation of the time-dependent cluster size distribution function, f_n, from a set of coupled linear differential equations:

$$\frac{df_n}{dt} = \omega^+_{n-1,n} f_{n-1} + \omega^-_{n+1,n} f_{n+1} - \left(\omega^+_{n,n+1} + \omega^-_{n,n-1}\right) f_n, \tag{1}$$

which describe reactions of attachment and detachment of single molecules ("structural units") to or from clusters of a new phase. The subscript n denotes the number of "structural units" with a characteristic size d_0 in the crystalline cluster, ω^+ and ω^- are attachment and detachment rates, $\omega^+_{n,n+1}$ is the rate that a cluster made up of n structural unities gains another to become an $n+1$ cluster, and $\omega^-_{n,n-1}$ the rate that it loses one unity to become a $n-1$ cluster,

$$\omega^+_{n,n+1} = K_s \frac{n^{2/3}}{d_0^2} D \begin{cases} 1 & \text{for } n \geq n_{cr} \\ \exp\left(-\frac{W_{n+1}-W_n}{k_B T}\right) & \text{for } n < n_{cr} \end{cases} \tag{2}$$

$$\omega^-_{n,n-1} = \omega^+_{n-1,n} \exp\left(\frac{W_n - W_{n-1}}{k_B T}\right), \tag{3}$$

where $K_s = (36\pi)^{1/3}$ is the shape factor for spherical clusters, D is the effective diffusivity controlling nucleation, and W_n is the work of cluster formation made up of n structural unities,

$$W_n = n\Delta\mu + K_s d_0^2 \sigma n^{\frac{2}{3}}, \tag{4}$$

where

$$\Delta\mu = \mu_s - \mu_l = -d_0^3 \Delta G_V(T) \tag{5}$$

is the difference between the chemical potential of the structural units in the solid and liquid phases, $\Delta G_V(T)$ is the difference of Gibbs free energy per unit volume of same structural units in the liquid and solid phases, which gives the thermodynamic driving force for crystallization, σ is the specific energy of the interface between the cluster and the supercooled liquid, and d_0 is a characteristic size of the structural units, estimated as $d_0 \simeq \sqrt[3]{\frac{V_M}{N_A}} = 0.588$ nm, where V_M is the crystal molar volume and N_A is the Avogadro number.

W_n reaches a maximum at a critical size

$$n_{cr} = \frac{32\pi}{3}\left(\frac{\sigma}{d_0 \Delta G_V}\right)^3. \tag{6}$$

For $n < n_{cr}$ most clusters dissolve, whereas for $n > n_{cr}$ they tend to grow.

For an in-depth analysis of the nucleation experiment and in particular for calculating the distribution function f_n, it is necessary

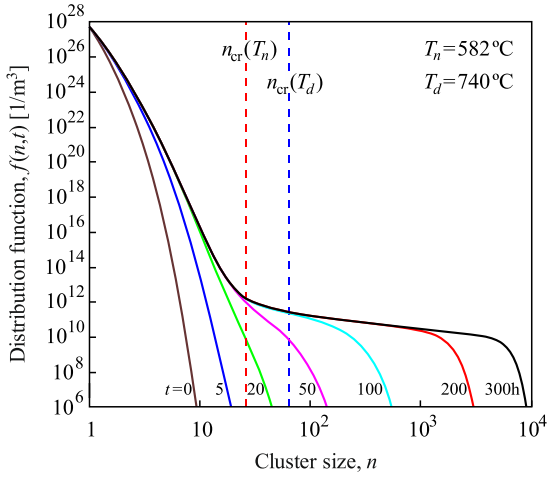

Fig. 4. Calculated cluster size distributions for glass D33 at $T_n = 582$ °C for different time-periods. The vertical lines denote the critical sizes at the nucleation and development temperatures.

to know the thermodynamic driving force for phase transition as a function of temperature. Since in the present work we deal with non-stoichiometric crystallization, the following formula derived in [15] was used,

$$\Delta G_V(x) = \Delta G_V^0(T) - \Delta G_V^0(T_L(x)) + \frac{k_B(T - T_L(x))}{d_0^3} \ln(1-x), \quad (7)$$

where x is the molar fraction of the second component (in our case, devitrite) that characterizes the deviation from stoichiometry (recall that we studied the nucleation and growth of combeite crystals). To use Eq. (7), one needs only the thermodynamic driving force $\Delta G_V^0(T)$ for crystallization at the stoichiometric composition ($x = 0$) and the liquidus temperature as a function of composition, $T_L(x)$. For $T_L(x)$, we used the polynomial fit given by Eq. (8) to experimental data shown as a solid line in Fig. 6c.

$$T_L(x) = \begin{cases} 1555 - 38x - 85x^2, & x \le 0.33 \\ 1603 - 69(1-x) - 54(1-x)^2, & x > 0.33 \end{cases} \quad (8)$$

For example, Fig. 4 shows the cluster size distribution functions for glass D33 after different time-periods at 582 °C.

Using the cluster size distribution functions and assuming an infinitely high heating rate from T_n to T_d, one may estimate the number densities of crystals nucleated after a time t at T_n ($n > n_{cr}(T_n)$):

$$N_n(t) = \sum_{n_{cr}(T_n)}^{\infty} f(n,t), \quad (9)$$

and after the development treatment at T_d ($n > n_{cr}(T_d)$):

$$N_d(t) = \sum_{n_{cr}(T_d)}^{\infty} f(n,t). \quad (10)$$

Then, to compute the steady-state nucleation rates, I_{st}, together with the respective induction times, we looked for the best fit of $N_d(t)$ to the experimental data letting the interfacial energy, σ, and the effective diffusivity, D, as *fitting* parameters. In this case, any fitting procedure (least-square, for example) of the $N(t)$ dependence would be very time-expensive, that is why we used a manual fitting. The $N(t)$ curves corresponding to the minimum, mean and maximum nucleation rates were fitted to the experimental data for each temperature. The fitted values of I_{st}, D, σ for the minimal and maximal nucleation rates were used to estimate the error.

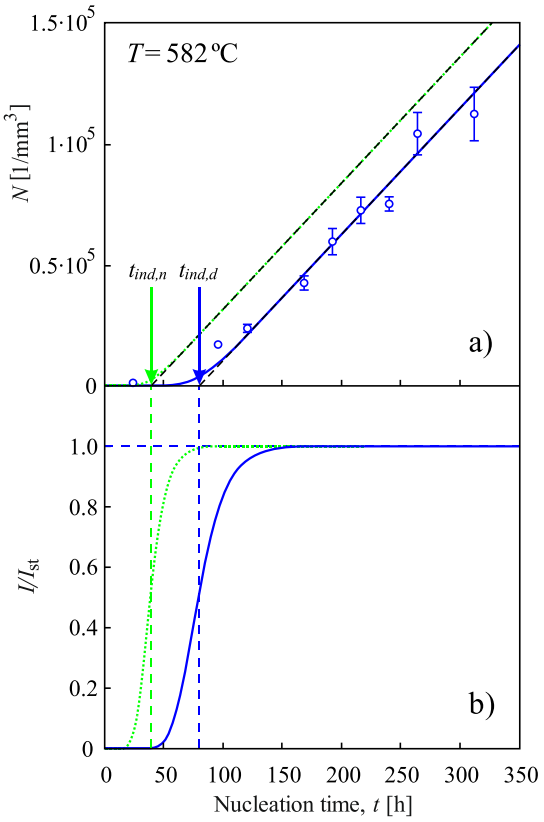

Fig. 5. a) The lines are the calculated number densities of supercritical clusters in the D33 glass versus nucleation time, t, at $T_n = 582$ °C, N_n (dotted line), and after development at $T_d = 740$ °C, N_d (solid line). The points refer to the experimental values of N_d. The dashed lines show the asymptotes of the dependencies of N on t. b) Evolution of the reduced nucleation rate, $(t)/I_{st} = \frac{dN}{dt}/I_{st}$, calculated from the N vs. t curves, such as those shown in (a).

Fig. 5a shows N vs. t dependencies calculated after nucleation (N_n) and development (N_d) treatments together with experimental data for N_d. As we showed in ref. [15] for other compositions, the development procedure shifts the $N(t)$ curve towards longer times, but does not affect the steady-state nucleation rate, I_{st}. This shift is due to the dissolution of a fraction of clusters larger than the critical size at T_n but did not grow enough to reach the critical size at T_d. The asymptotes of $N_n(t)$ and $N_d(t)$ intersect the time axis in the induction periods, $t_{ind,\,n}$ and $t_{ind,\,d}$, respectively, noting that $t_{ind,\,d}$ is the experimental induction time (which depends on the nucleation and development temperatures, and also on the heating rate from the nucleation to the development temperature), whereas $t_{ind,\,n}$ is the calculated intrinsic nucleation induction time.

Fig. 5b shows the nucleation rates $I(t) = dN/dt$ corresponding to the dotted and solid lines in Fig. 5a, normalized to their steady-state values I_{st}, for the cases of nucleated-only and developed crystals, respectively. The value of $I(t)$ increases with time, approaching the steady-state value, I_{st}.

4. Results and discussion

4.1. Glass properties and liquidus temperatures

Fig. 6a, b, c show, respectively, the room-temperature density of the glasses, the glass transition and the liquidus temperatures determined by DSC on heating at 10 °C/min for samples of different compositions in the interval from combeite ($x = 0$) to devitrite ($x = 1$).

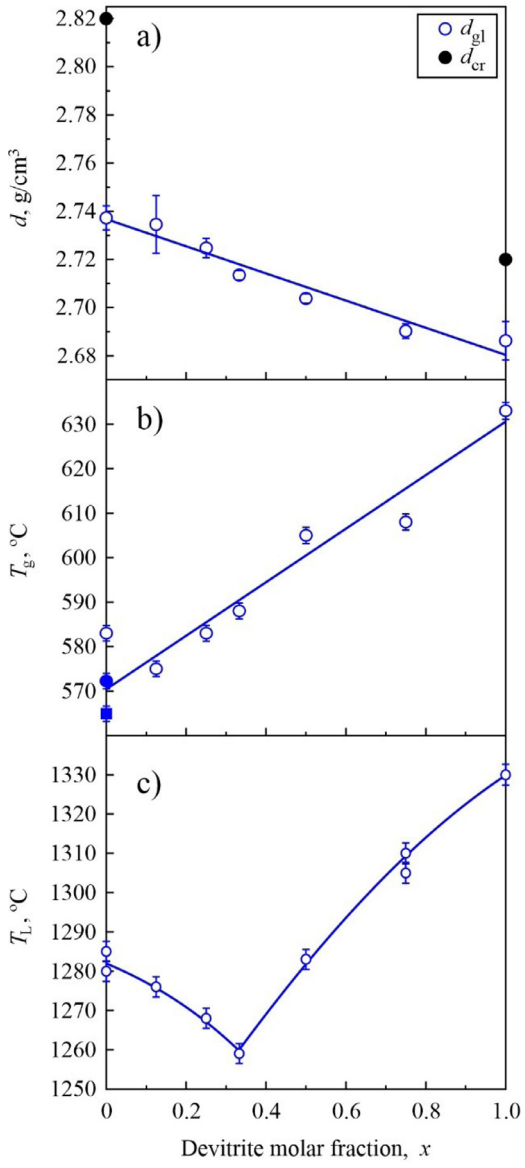

Fig. 6. (a) Density versus composition of glasses (d_{gl}) and crystalline (d_{cr}) combeite ($x = 0$) [20] and devitrite ($x = 1$) [21] at room temperature, (b) glass transition temperature: open symbols – this work, • – from [8], ■ – from [6], and (c) liquidus temperature determined by DSC on heating at 10°C/min. The solid lines in (a) and (b) are linear fits to the data points to guide the eyes. The solid line in (c) is the best polynomial fit according to Eq. (8).

Fig. 6a shows the glass density increases as x decreases. The calculated densities from atomic structure information determined by X-ray diffraction of combeite and devitrite crystals are also shown in Fig. 6a [20, 21].

An increase in devitrite content x is also accompanied by an approximately linear growth of the glass transition temperature (Fig. 6b), which is associated with an increase in the number of bridging oxygens in the silicon-oxygen network. The latter can be evaluated by the ratio of silicon to oxygen atom number $f_{si} = N_{Si}/N_O$ [22]. Indeed, as can be seen in Fig. 7, T_g increases by increasing f_{si}.

However, f_{si} is not the only factor that affects the glass transition temperature. For example, for compositions in the pseudo-binary metasilicates $Li_2O{\bullet}SiO_2$–$CaO{\bullet}SiO_2$ [13] and disilicates $Li_2O{\bullet}2SiO_2$–$BaO{\bullet}2SiO_2$ joints [15] with constant $f_{si} = 1/3$ and

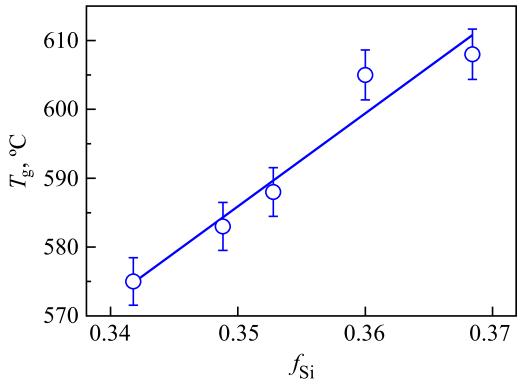

Fig. 7. Glass transition temperature versus $f_{si} = N_{Si}/N_O$, the number of silicon to the number of oxygen atoms.

2/5, respectively, the glass transition temperature exponentially increases by increasing the glass density.

It should be noted in Fig. 6a that the relative density difference $\Delta d = (d_{cr} - d_{gl})/d_{gl}$ between the glass and the corresponding crystal is lower for devitrite ($\Delta d = 0.018$) than for combeite ($\Delta d = 0.030$), i.e., the melting of devitrite crystals results in a smaller increase in volume than that of combeite crystals. It is possible that this fact and the great network connectivity, explain the higher T_g of glass D100 than glass D0.

According to Fig. 6c, the liquidus temperature $T_L(x)$ has a minimum for the D33 glass. We need $T_L(x)$ to estimate the thermodynamic driving force for crystallization using Eq. (7). It is important to note that the combeite-devitrite joint is not a real binary system. A DSC curve of the D33 glass indicates the melting of three phases (see Fig. S2 in Supplementary material), however, an analysis of their precipitation sequence is not within the scope of this article.

4.2. Crystal nucleation

The calculated number densities of crystals per unit volume, N, as a function of the nucleation time, after a developing treatment, as shown in Fig. 5, are presented in Supplementary material for glasses D0, D25, and D33 (Figs. S3, S4 and S5 in Supplementary material) together with experimental data. According to an XRD analysis (see Fig. S1 in Supplementary material), the only crystal phase present is combeite. To achieve the best agreement between experimental data and the calculated $N(t)$, the diffusivity, D, and the nucleus/liquid specific interfacial energy, σ, were left as fitting parameters. Their values are shown in Figs. 8 and 9 for D0, D25, and D33 glasses. Figs. 8a and 9 show that the interfacial energy increases as the crystal composition moves away from that of the precursor glass.

Above the temperature of the maximum nucleation rate, T_{max}, a linear function of T can fit the interfacial energy [2], with the coefficients depending on composition,

$$\sigma(T,x) = 0.04214 - 0.0005643x + 0.01254x^2 + 10^{-5}(8.083 + 1.455x)T \ \left[\mathrm{J/m^2}\right]. \quad (11)$$

Regarding the diffusion coefficient, to facilitate the data analysis, we used a fitting function $D(T, x)$, of Arrhenius form

$$D(T,x) = D_0(x)\exp\left[-\frac{90,000}{T}\right], \quad (12)$$

where $D_0(x)$ is a composition-dependent pre-exponential factor equal to

$$D_0(x) = 7.777 \cdot 10^{23}\exp\left(-2.5x - 83x^3\right) \ \left[\mathrm{m^2/s}\right].$$

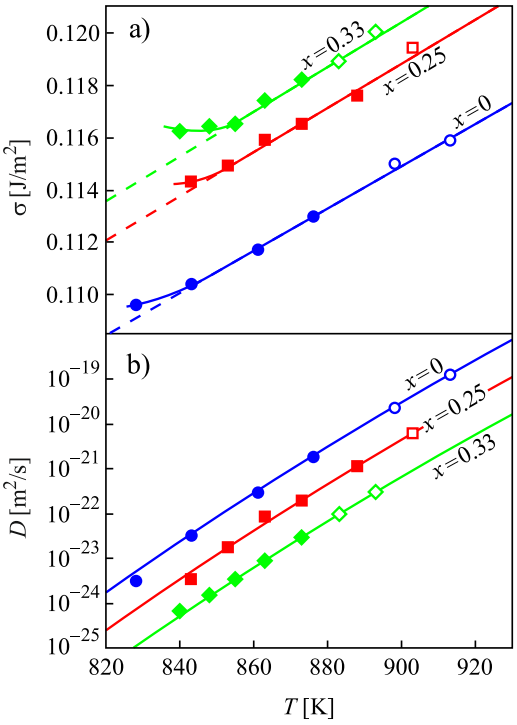

Fig. 8. a) Nucleus/liquid interfacial energy for glasses D0 ($x = 0$), D25 ($x = 0.25$) and D33 ($x = 0.33$) versus temperature. The points were calculated as fitting parameters from the best fit of $N(t)$ given by Eq. (10) to experimental data. Open symbols were calculated with extrapolated data. The dashed lines were drawn considering a linear $\sigma(T)$, Eq. (11), on fitting. The solid lines were calculated assuming a deviation of $\sigma(T)$ from the linear approximation (see details in [23, 24]). b) Diffusion coefficients as a function of temperature. The points (solid symbols) were calculated by fitting $N(t)$ to experimental data; open symbols are extrapolated according to Arrhenius dependencies Eq. (12), which are shown by the solid lines. Error bars are less than symbol size.

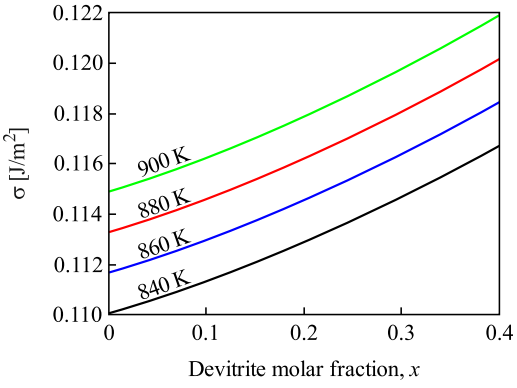

Fig. 9. Nucleus/liquid specific interfacial energy versus precursor glass composition, x (devitrite molar fraction) according to Eq. (11), for different temperatures in the range of maximum nucleation rate.

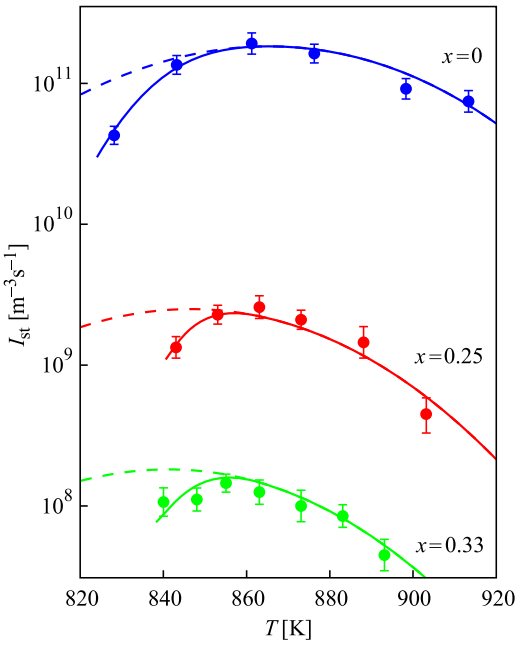

Fig. 10. Steady-state nucleation rates, $I_{st}(T)$, computed from $N(t)$ curves for different temperatures and molar fractions, x, of $Na_2O{\bullet}3CaO{\bullet}6SiO_2$ (devitrite). The dashed lines were calculated from fitting experimental $N(t)$ curves by Eq. (10), with a linear dependence of $\sigma(T)$ given by Eq. (11). The solid lines were calculated assuming the deviation of $\sigma(T)$ from the linear approximation at low temperatures, as shown in Fig. 8a.

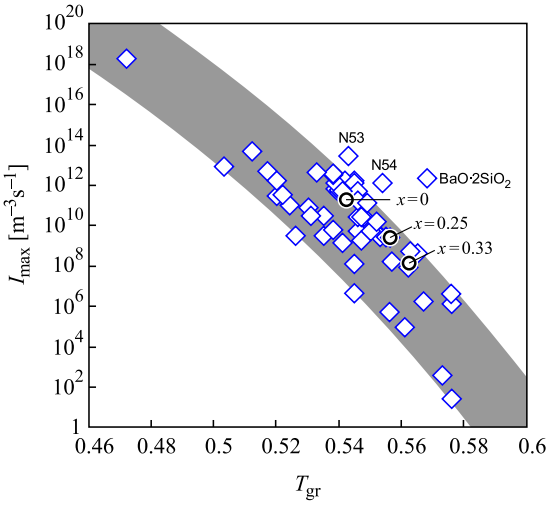

Fig. 11. Maximum steady-state nucleation rate versus reduced glass transition temperature for several stoichiometric and non-stoichiometric silicate glasses that show homogeneous nucleation [17]. The circles added here correspond to the glasses D0 (x=0), D25 (x=0.25), and D33 (x=0.33) of this study.

Fig. 10 shows the steady-state nucleation rates, determined as $I(T) = dN/dt$ of the simulated $N(t)$ (Fig. 7), at different nucleation temperatures for glasses D0, D25, and D33.

It follows from Fig. 10 that the steady-state nucleation rate of combeite crystals strongly drops when the glass composition deviates from the combeite stoichiometry ($x = 0$). The maximum steady-state nucleation rate, I_{max}, decreases as the reduced glass transition temperature $T_{gr} \equiv T_g/T_l$ increases, confirming a well-known trend: the higher T_{gr}, the lower the steady-state nucleation rate maximum. This behavior is shown in Fig. 11 for different silicate glasses and the three glasses studied here: D0 ($x = 0$), D25 ($x = 0.25$), and D33 ($x = 0.33$). A decrease in the maximum steady-state nucleation rate of combeite crystals by approximately three orders of magnitude when x varies from 0 up to 0.33 is due to the increase in σ (Fig. 8a), and hence the increase of thermodynamic barrier for nucleation, and a decrease in D (Fig. 8b). Note that a reduction in D diminished the nucleation rate by approximately two orders of magnitude.

Depending on the glass, the increased difference between the glass composition and the precipitating crystalline phase can decrease or increase the diffusion coefficient (e.g., [13, 8]). In contrast to diffusion, any increase in the compositional mismatch between the crystal and the supercooled liquid increases the interfacial en-

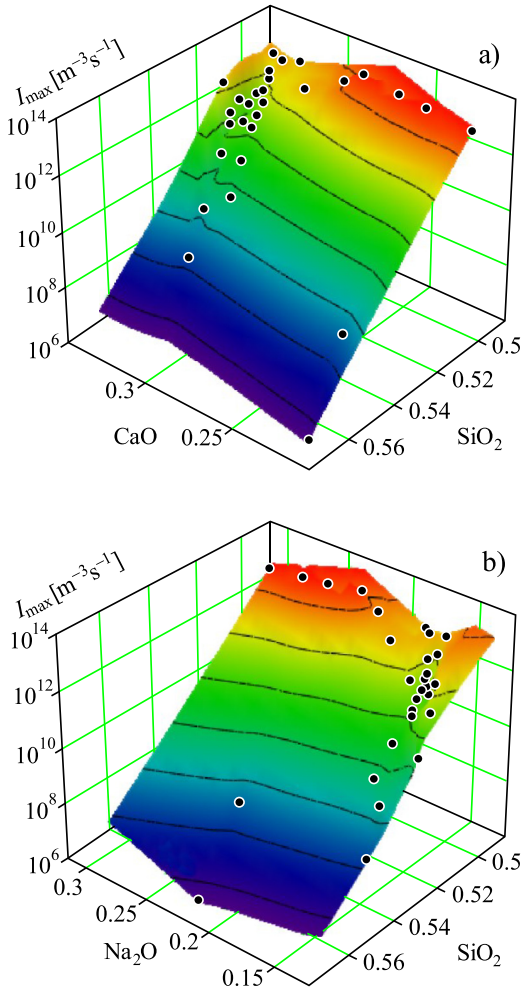

Fig. 12. I_{max} as a function of glass composition (mole fractions) in the soda-lime-silica system. The points refer to our experimental data and other data taken from [5–8,14].

ergy, as shown in Fig. 9, and also in our previous publications for other systems [13, 15]. Finally, the thermodynamic driving force decreases with a deviation from stoichiometry for all considered systems [13, 15]. The interplay of these changes in diffusion, interfacial energy, and thermodynamic driving force determines how the nucleation rate will vary with a deviation of the precursor glass composition from that of the precipitating crystal.

In Fig. 12, we collected different literature data of maximum nucleation rates, I_{max}, versus composition for glasses of the Na_2O–CaO–SiO_2 system together with our measurements.

Fig. 12 shows that an increase in silicon oxide content leads to a strong drop in nucleation rates. A decrease in the content of sodium oxide or an increase in the content of calcium oxide results in a weak decrease in the nucleation rate. These trends are reasonable and already known. However, it is unexpected and very interesting that all the 29 experimental points lay not more than 1 o.m. within the interval $\log(I_{max}) = 6.6 \ldots 13.7$ on a flat surface described by the following equations:

$$\log\left(I_{max}\left(C_{Na_2O},\ C_{SiO_2}\right)\right) = 14.7C_{Na_2O} - 76.6C_{SiO_2} + 47.8 \quad (13a)$$

or

$$\log\left(I_{max}\left(C_{CaO},\ C_{SiO_2}\right)\right) = 62.6 - 14.7C_{CaO} - 91.3C_{SiO_2}, \quad (13b)$$

where I_{max} is the maximum steady-state nucleation rate in m^{-3}s^{-1}, and C is the mole fraction of the corresponding oxides. The above equations allow estimates of I_{max} for any given glass composition of the Na_2O–CaO–SiO_2 system with reasonable accuracy. Taking into account the difficulties related to the experimental determination of nucleation rate data, such an assessment can be very useful.

4.3. Crystal growth

Fig. 13 show the dependences of the radii R of combeite crystals on the growth time at different temperatures in glasses D0, D25, and D33. We used the simple normal growth model to estimate the effective diffusion coefficient D_U from experimental crystal growth rate data, determined as

$$U = \frac{dR}{dt}. \quad (14)$$

According to the normal growth model (e.g., [25]), at deep undercooling,

$$U = \frac{D_U}{4d_0}. \quad (15)$$

Coefficients D_U defined in this way are shown in Fig. 14 as a function of temperature for glasses D0, D25, and D33. For comparison, we replot the diffusion coefficient, D, from the crystal nucleation fits. Recall that D governs the formation of crystalline clusters with nanoscale sizes, including the critical cluster size, unlike D_U, which is responsible for the deterministic growth of macroscopic (micron-scale size) crystals.

Using the Normal Growth model leads to the minimum values of the diffusion coefficient calculated from experimental growth rates. This method estimates the lowest temperatures $T_{n/U}$ at which D and D_U converge. In our case, $T_{n/U}$ varies approximately from 920 to 970 K for glasses D0 to D33, respectively. However, for most silicate crystals, having high melting entropy, ΔS_m (e.g., $\Delta S_m \approx 8R$ for combeite crystal), the Screw Dislocation model is more probable. According to this model, the crystal growth rate at high supercoolings can be written as

$$U = f\frac{D_U}{4d_o}, \quad (16)$$

where

$$f \cong \frac{1}{2\pi}\frac{(T_m - T)}{T_m} \quad (17)$$

is a dimensionless parameter [26].

Using Eq. (16) at high undercooling (our case) practically does not affect the effective activation energy (f changes weakly), but increases the value of D_U by a factor $1/f$ that for glasses D0, D25, and D33 is about 14, increasing the temperature $T_{n/U}$, from which it is reasonable to assume the proximity of D and D_U. Although according to Fig. 14, the temperature ranges of experimental nucleation and growth rates overlap only slightly, it is evident that below $T_{n/U}$ the apparent activation energies and pre-exponentials for D and D_U are sturdily different, hence $D_U \gg D$.

These results corroborate our previous studies on glasses of different systems and compositions ($Li_2O{\cdot}2SiO_2$ & $Na_2O{\cdot}2CaO{\cdot}3SiO_2$) [27], $Li_2O{\cdot}2SiO_2$–$BaO{\cdot}2SiO_2$ [15]). The increasing difference, $D_U \gg D$, at low temperatures, was clearly shown for a stoichiometric $Li_2O{\cdot}2SiO_2$ glass. This difference at low temperatures can be related to another long-known fact: at temperatures close to the temperature T_{max} of maximum nucleation rate, and especially below it, the induction periods of nucleation t_{ind} are much shorter than the period during which crystal growth is not observed, t_U (e.g., [28–30]). In our case, for glass D33, t_U at 620°C is about 30 h (Fig. 13d), whereas t_{ind} at the same temperature is only 1 h (Fig. S5). It should be noted that this difference is detected only at temperatures lower than $T_{n/U}$. Even though the above fundamental problem – $t_{ind} \ll t_U$ – was first claimed more than 20 years

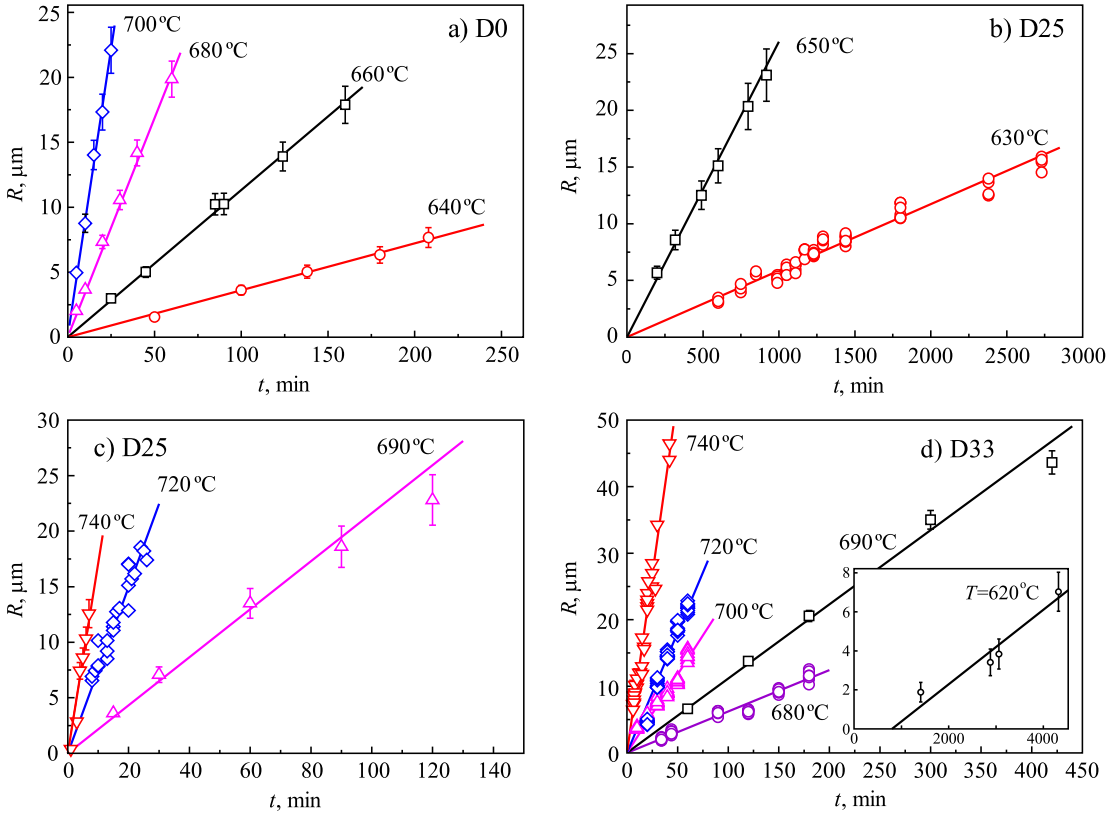

Fig. 13. Radius of spherulitic combeite crystals as a function of growth time in glasses of different compositions for different growth temperatures (a) D0, (b) D25 nucleated at 600°C for 3 h, (c) D25 nucleated at 600°C for 3 h, (d) D33 nucleated at 582°C for 120 h.

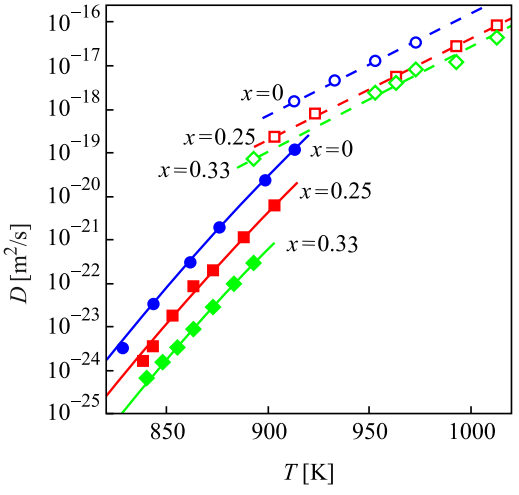

Fig. 14. Effective diffusion coefficients estimated from the growth rates of macroscopic crystals, D_U, via Eq. (14) (open symbols), and from nucleation kinetics of nanometric clusters, D (Fig. 8b) (closed symbols) for three glass compositions.

ago [28], it remains unresolved, and its solution would require a more in-depth investigation using new experimental data and techniques. However, a thorough study of this challenging problem is outside the scope of this article.

5. Conclusions

We clearly showed that as the precursor-glass composition shifts from combeite to devitrite, the maximum steady-state nucleation rate of combeite crystals, $I_{st}(T_{max})$, strongly drops. Based on this work, and our previous results with three other oxide systems, we propose that the deviation of the glass composition from the stoichiometry of the precipitated crystals leads to a diminished driving force, ΔG, and increased nucleus/liquid interfacial energy, σ, which significantly decrease the nucleation rates. However, the diffusion coefficient, D, can increase or decrease, depending on the glass-forming system (e.g., [8, 13]).

Finally, we also discovered a significant difference between the diffusion coefficients calculated from nucleation and growth rates, which are most clearly revealed at relatively low temperatures, approaching T_g. This is an important open issue, also reported for other systems. The reasons for this difference in the growth kinetics of crystalline nanoclusters (nucleation) and microscopic crystals (growth) warrant further work.

Taken *in toto*, the overall results of this research significantly contribute to shedding light on the complex crystallization kinetics of non-stoichiometric glasses, the most common commercial glasses.

Declaration of Competing Interest

The authors declare that they have no known competing financial interests or personal relationships that could have appeared to influence the work reported in this paper.

Acknowledgments

This research was supported by the University of São Paulo, Brazil, for a Visiting Researcher Fellowship (V.M.F., grant 2016.1.1376.18.4). We are also grateful for the support from CNPq and the São Paulo Research Foundation – FAPESP – CeRTEV grants 2013/07793-6 and 2019/02396-5. This study was financed in part

by the Coordenação de Aperfeiçoamento de Pessoal de Nível Superior – Brasil (CAPES) – Finance Codes 001 and 88887.468838/2019-00 (VMF).

Supplementary materials

Supplementary material associated with this article can be found, in the online version, at doi:10.1016/j.actamat.2020.06.039.

References

[1] J. Deubener, M. Allix, M.J. Davis, A. Duran, T. Höche, T. Honma, T. Komatsu, S. Krüger, I. Mitra, R. Müller, S. Nakane, M.J. Pascual, J.W.P. Schmelzer, E.D. Zanotto, S. Zhou, Updated definition of glass-ceramics, J. Non-Cryst. Solids 501 (2018) 3–10.
[2] K.F. Kelton, A.L. Greer, Nucleation in condensed matter. Applications in Materials and Biology, Pergamon Mater. Series (2010) 276.
[3] W. Höland, G. Beall, Glass-Ceramic Technology, American Ceramic Society, 2002.
[4] D.G. Barnett, R.W. Douglas, Nucleation and crystallization in the soda-baria-silica system, Phys. Chem. Glasses 12 (1971) 117–124.
[5] Z. Strnad, R.W. Douglas, Nucleation and crystallization in the soda-lime-silica system, Phys. Chem. Glasses 14 (1973) 33–36.
[6] C.J.R. Gonzales-Oliver, P.F. James, Crystal nucleation and growth in a $Na_2O•2CaO•3SiO_2$ glass, J. Non-Cryst. Solids (1980) 699 C.J.R. Gonzalez-Oliver, Crystal Nucleation and Growth in Soda-Lime-Silica Glasses, the University of Sheffield, Sheffield, 1979. Ph.D. Thesis.
[7] K. Lakshmi Narayan, K.F. Kelton, First measurements of time-dependent nucleation as a function of composition in $Na_2O•2CaO•3SiO_2$ glasses, J. Non-Cryst. Solids 200 (1997) 222–230.
[8] O.V. Potapov, V.M. Fokin, V.L. Ugolkov, L. Ya, Suslova, V.N. Filipovich, Influence of Na_2O content on the nucleation kinetics in glasses of compositions close to the $Na_2O•2CaO•3SiO_2$ stoichiometry, Glass Phys. Chem. 26 (2000) 27–32.
[9] E.G. Rowlands, P.F. James, Nucleation and crystal growth in the lithia-baria-silica system, in: Proceedings of the International Congress on Glass, Volume 2. Extended Abstracts, Edinburgh, Scotland, 2001 1-6 July.
[10] V.M. Fokin, N.S. Yuritsyn, O.V. Potapov, B.A. Shakhmatkin, N.V. Vedisheva, V.L. Ugolkov, A.G. Cherepova, Nucleation of crystals in lithium-silicate glasses, Russ. J. Phys. Chem. 77 (2003) 146–148.
[11] M.F. Barker, Tian-He Wang, P.F. James, Nucleation and growth kinetics of lithium disilicate and lithium metasilicate in lithium-silica glasses, Phys. Chem. Glasses 29 (1988) 240–248.
[12] V.M. Fokin, E.D. Zanotto, Continuous compositional changes of crystal and liquid during crystallization of a sodium calcium silicate glass, J. Non-Cryst.Solids 353 (2007) 2459–2468.
[13] V.M. Fokin, R.M.C.V. Reis, A.S. Abyzov, C.R. Chinaglia, E.D. Zanotto, Nonstoichiometric crystallization of lithium metasilicate–calcium metasilicate glasses. Part 1 — Crystal nucleation and growth rates, J. Non-Cryst. Solids 362 (2013) 56–64.
[14] N.S. Yuritsyn, Nucleation of crystals in sodium calcium silicate glasses of the metasilicate section, Glass Phys. Chem. 41 (2015) 112–115.
[15] V.M. Fokin, A.S. Abyzov, A.M. Rodrigues, R.Z. Pompermayer, G.S. Macena, E.D. Zanotto, E.B. Ferreira, Effect of non-stoichiometry on the crystal nucleation and growth in oxide glasses, Acta Mater. 180 (2019) 317–328.
[16] A.M. Kalinina, V.N. Filipovich, V.M. Fokin, Stationary and non-stationary crystal nucleation rate in a glass of $2Na_2O•CaO•3SiO_2$ stoichiometric composition, J. Non-Cryst. Solids (1980) 723–728.
[17] A.S. Abyzov, V.M. Fokin, E.D. Zanotto, Predicting homogeneous nucleation rates in silicate glass-formers, J. Non-Cryst. Solids 500 (2018) 231–234.
[18] V.M. Fokin, E.D. Zanotto, N.S. Yuritsyn, J.W.P. Schmelzer, Homogeneous crystal nucleation in silicate glasses: A 40 years perspective, J. Non-Cryst. Solids 352 (2006) 2681–2714.
[19] R.T. DeHoff, Quantitative Microscopy, McGraw-Hill Book Company, 1968.
[20] I. Maki, T. Sugimura, Metasilicates in ternary system Na_2O-CaO-SiO_2, J. Ceram. Assoc. Jpn 76 (1968) 16–20.
[21] IEM Databases and Datasets, Card No: 10288.
[22] A.A. Appen, Glass chemistry, Publishing house Chemistry, Leningrad Branch (1970).
[23] V.M. Fokin, A.S. Abyzov, E.D. Zanotto, D.R. Cassar, A.M. Rodrigues, J.W.P. Schmelzer, Crystal nucleation in glass-forming liquids: Variation of the size of the "structural units" with temperature, J. Non-Cryst. Solids 447 (2016) 35–44.
[24] A.S. Abyzov, V.M. Fokin, N.S. Yuritsyn, A.M. Rodrigues, J.W.P. Schmelzer, The effect of heterogeneous structure of glass-forming liquids on crystal nucleation, J. Non-Cryst. Solids 462 (2017) 32–40.
[25] J.W. Christian, The Theory of Transformations in Metals and Alloys, Part I, Oxford, Pergamon, 1981.
[26] D.R. Uhlmann, Crystal growth in glass forming system: a ten years perspective. In *Advances in ceramics, Volume 4. Nucleation and crystallization in glasses*.1982. Edited by J.H. Simmons, D.R. Uhlman & G.H. Beall. American Ceramic Society. Columbus. Ohio. P. 80–124.
[27] V.M. Fokin, J.W.P. Schmelzer, M.L.F. Nascimento, E.D. Zanotto, Diffusion coefficients for crystal nucleation and growth in deeply undercooled glass-forming liquids, J. Chem. Phys. 126 (2007) 234507.
[28] J. Deubener, R. Brückner, M. Sternitzke, Induction time analysis of nucleation and crystal growth in di- and metasilicate glasses, J. Non-Cryst. Solids 163 (1993) 1–12.
[29] V.M. Fokin, N.S. Yuritsyn, E.D. Zanotto, J.W.P. Schmelzer, A.A. Cabral, Nucleation time-lag from nucleation and growth experiments in deeply undercooled glass-forming liquids, J. Non-Cryst. Solids 354 (2008) 3785–3792.
[30] A.M. Rodrigues, D.R. Cassar, V.M. Fokin, E.D. Zanotto, Crystal growth and viscous flow in barium disilicate glass, J. Non-Cryst. Solids 479 (2018) 55–61.